# Design and Performance Analysis of Massive MIMO Modeling with Reflected Intelligent Surface to Enhance the Capacity of 6G Networks

**Hyakanur Basavanna Mahesh**
Department of Computer Science & Engineering, PES University, India | Visvesvaraya Technological University, India
hbmahesh@gmail.com

**Guttur Fakruddin Ali Ahammed**
Department of Computer Science & Engineering, PG Center, Visvesvaraya Technological University, India
aliahammed78@gmail.com

**Shiramally Mallappa Usha**
Department of Electronics & Communication Engineering, JSS Academy of Technical Education, India
ushasm@jssateb.ac.in (corresponding author)

*Received: 27 July 2023 | Revised: 7 September 2023 | Accepted: 23 September 2023*

 *DOI: https://doi.org/10.48084/etasr.6234*

## ABSTRACT

**Reflected Intelligent Surface (RIS) can establish a virtual line-of-sight link to enhance system performance while consuming less power in non-line-of-sight. RIS technique is utilized to minimize the spreading of electromagnetic signals by modifying the surface's electric and magnetic field characteristics. RIS can be adopted with the existing environment to effectively increase efficiency by modifying the radio channel characteristics. The signals are steered to the receiver using an RIS thus improving the link quality. The radio channel is viewed in traditional wireless systems as an uncontrollable entity that typically tampers with transmitted signals. This paper suggests an alternate theoretical model after examining the prevalent models and potential issues. Security of the wireless communication physical layer can be improved with an RIS by just changing the phase of the reflective unit. In this work, the massive Multiple Input Multiple Outputs (MIMO)-based iterative modeling technique is used to build the transmitter, channel, and receiver section. This will simultaneously optimize the RIS passive beamforming pre-coding matrix and thus avoid multi-user interference. At the base station cyclic programming is adopted, it iteratively calculates the active and passive beam-forming RIS matrices. The simulation results demonstrate that the combined pre-coding technique used in this work improves the weighted sum rate, efficiency, and coverage ratio. The results show that MIMO with continuous phase shift RIS achieves a higher Weighted Sum Ratio (WSR) and minimum Channel State Information (CSI) error in comparison with the random phase shift RIS. The performance metrics sum rate, signal-to-interference plus noise ratio (SINR), energy efficiency, and transmit power are analyzed and compared.**

***Keywords-RIS; 6G Networks; massive MIMO; CSI; WSR***

## I. INTRODUCTION

The majority of operators are interested in the 6G wireless network due to its technological benefits such as the efficiency in the frequency spectrum, energy efficiency, low latency, and high coverage. The 6G wireless network depends on effective energy management and power efficiency. Security in communication is an important criterion to be considered along with energy efficiency. In wireless communication, security can be provided in two ways [1]. The conventional technology uses software and hardware data encryption at the physical layer level. It performs well to safeguard the data without adding any extra overhead. A Reflected Intelligent Surface (RIS) can be used to provide the security at the physical layer. Due to the advancement of RIS, wireless communication systems gain a unique dimension.

## II. RELATED WORK

In [2], the design challenges of an RIS-assisted Single-Output (MISO) system's beam were explored. The complex beam forming techniques for imperfect channels were analyzed in [3]. Authors in [4] investigated the impact of deploying networks using the RIS structure. Downlink deployment of the network using an RIS can maximize the signal power but in-turn increases the interference level. Authors in [5] investigated the optimal passive beam and active beam forming vector of a Base Station (BS) to enhance the weighted sum of downlink rates. The corresponding weight represents the mobile user priority to access the base station. In [6], the authors achieved low-cost delay for end-to-end multiple downlink path. In [7, 8], latency minimization in 6G networks is achieved with efficient Routing Strategy. In order to achieve promising performance in loaded settings, a number of detectors for large MIMO systems are presented in [8-12]. The main goal is to enhance the detector's performance by identifying any hidden sparsity in the received signal's residual error. The symbol error vector acquired from a linear detector is used in the first stage to transform the standard MIMO model into the sparse model. Recent research in the field of massive Multiple Input Multiple Output (MIMO) antennas shows that user channels improve as the number of BS antennas increases, allowing high signal amplification with minimal inter-user interference [13]. An Ultra Wide Band (UWB) MIMO receiving wire working at millimeter-wave is proposed in [14-16]. It is made out of 8 transmitting components with different shapes. It is planned with a rectangular construction and different cut spaces. The proposed plan covers the total super wideband for short remote frameworks.

## III. MASSIVE MIMO DOWNLINK MODEL AND PROBLEMS

The RIS structure shown in Figure 1 consists of an Intelligent Reflecting Surface (IRS), a controller, a BS, a legitimate receiver, and an eavesdropper. An RIS is a low-cost reflecting device. The gain and intensity of the signal is adjusted by tuning the phase angle of the reflected signal. If the phase difference between the signals is one bit period, then the signal arrives simultaneously to the receiver [8]. The system is having the capacity to cope with the multiple concurrent signals arriving simultaneously towards the receiver. Here the relative delay is maintained among the signals which are arriving towards the reviver in order to avoid interference [8].

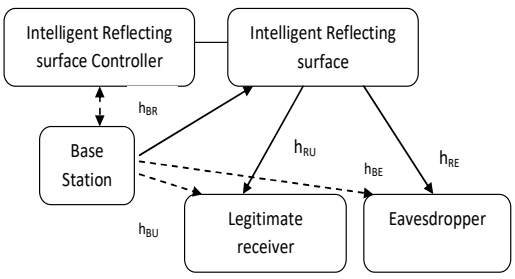


Fig. 1. MISO downlink model with RIS structure.

The channel co-efficient matrices are shown in (1)-(3):

$$h_{BR} \in C^{M \times N_t} \quad (1)$$

$$h_{BU} \in C^{1 \times N_t} \quad (2)$$

$$h_{RU} \in C^{1 \times M} \quad (3)$$

where $h_{BR}$ is the channel coefficient matrix from the BS to the RIS, $h_{BU}$ is the channel coefficient matrix from the BS to a legitimate user [9], and $h_{RU}$ is the channel coefficient matrix from to the RIS to the legitimate user, respectively [10-11]. A channel is estimated by analyzing the signal received from the receiver as shown in (4). The co-efficient matrix of the RIS is given in (5).

$$y_U = (h_{BU} + h_{RU} \Phi H_{BS}) fx + n_U \quad (4)$$

$$\Phi = \text{diag}(\beta_1 e^{j\theta 1}, \beta_2 e^{j\theta 2}, \beta_3 e^{j\theta 3} \ldots . \beta_M e^{j\theta M} \ldots . \quad (5)$$

where $\beta_k \in [0,1]$is the amplitude of the $k^{th}$ unit of an RIS and $\theta_k \in [0, 2\pi]$ is the phase of the $k^{th}$ unit of the RIS. The received signal from the eavesdropper is depicted by:

$$y_E = (h_{BE} + h_{RE} \Phi H_{BR}) fx + n_E \quad (6)$$

The coefficients $h_{RE}$ and $h_{BE}$ are given by:

$$h_{RE} \in C^{1 \times M} \quad (7)$$

$$h_{BE} \in C^{1 \times N_t} \quad (8)$$

where $h_{RE}$ and $h_{BE}$ represent the coefficient matrices from an reconfigurable intelligent surface to the private listener called eavesdropper and from the BS to the private listener respectively and $\eta_E$ represents the noise at the eavesdropper.

## IV. SYSTEM DESIGN

An IRS element is assumed to have components pointing upward and max elements on a level plane (M = May's Max). An IRS unit organizes the reflecting modes is controlled by the smart controller. The linear transmit precoding (TPC) matrix is utilized by the BS to communicate its information vector $S_k$ to the $k^{th}$ user. The following assumptions are made for the feasible set of RCs: f =diag(bq1...bqn),qn $\in$ [0, 2pi] and b $\in$ [0,1] are the diagonal phase-shift lattice of an IRS, the combined incident signal's phase shift, and the amplitude reflection coefficient respectively. The structure of the cellular free network consists of the RIS, BS, CPU, and users connected to the network as depicted in Figure 2. The users and BSs are linked through an RIS. BSs, RIS, and CPU are interlinked virtually. The downlink channel of an RIS-CF system is depicted in Figure 3. As shown, many RIS units and many BSs are linked to communicate with the user. An RIS receives the signal from the BS and reflects the same signal to the user.

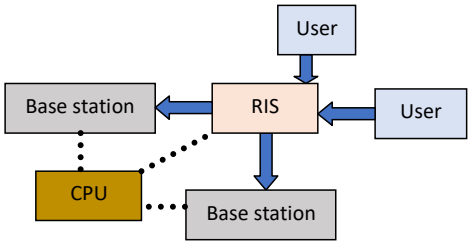


Fig. 2. Structure of a cellular-free network.

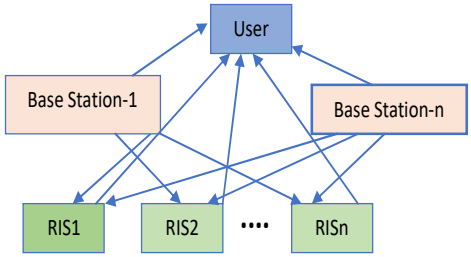


Fig. 3. Downlink channel of an RIS-CF system.

The distance between the users and the BS is reduced by incorporating RIS-CF, this way the gain is boosted by using massive MIMO cellular free networks. The above structure minimizes the resources.

### A. Transmitter Design

All the BSs must be synchronized and independent and should send the information through the unified channel to provide better services to all subscribers. Assume that as given below in (9):

$$D_n \triangleq [D_{n,1} \dots \dots \dots D_{n,m}]^T \in C^K \quad (9)$$

where D, k, and P represent the data to be transmitted, the $m^{th}$ number of users, and the $n^{th}$ subcarrier, respectively. The data in the downlink channel can be expressed in the frequency domain as:

$$Z_{bs,n} = \sum_{n=1}^{n} V_{bs,n,m} D_{n,m} \quad (10)$$

In (10), the pre-coding chosen vector is $V_{bs,n,m}$, where bs stands for base station, n represents the channel, and m indicates the user.

### B. Channel Design

The BS transmits the signal to an RIS unit and the user gets the reflected signals from an RIS. The channel is specified as:

$$ch^{CH}_{bs,n,m} \in C^{U \times M} \quad (11)$$

Equation (11) is rewritten in terms of BS user link and BS station RIS user link as shown in (12).

$$ch^{CH}_{bs,n,m} = CH^{H}_{bs,m,n} + \sum_{ris=1}^{R} E^{CH}_{ris,m,n} \odot^{CH}_{ris} G_{bs,ris,n} \quad (12)$$

where $CH^{H}_{bs,m,n} \in \mathbb{C}C^{U \times M}$ is the channel in frequency domain representation from the $bs^{th}$ BS to the $m^{th}$ user, $E^{CH}_{ris,m,n} \in \mathbb{C}C^{U \times N}$ is a channel established from an RIS to the $m^{th}$ user, $G_{bs,ris,n} \in \mathbb{C}C^{N \times M}$ is a channel established from a BS to an RIS, and $\Theta^{H}_{r} = \mathbb{C}C^{NXN}$ is a phase shift N×N matrix, defined by:

$$\Theta_r \triangleq \text{diag}(\theta_{r,1} \dots \dots \dots \theta_{r,N}), \forall_r \in \mathcal{R} \quad (13)$$

where $\theta_{r,N}$ belongs to F, it is a RIS reflection coefficient given by:

$$\mathcal{F} \triangleq \{\theta_{r,n} || \theta_{r,n} | \leq 1\}, \forall_r \in \mathcal{R}, \forall_n \in \mathcal{N} \quad (14)$$

### C. Receiver Design

The Alternating Direction Method of Multiplier (ADMM) algorithm is used to improve active and passive beam formation in terms of SINR, energy efficiency, and transmit power parameters. An IRS-aided system at the Access Point (AP) beats the massive MIMO without an IRS. It is assumed that the signal from the mobile user propagates along the channel path.

- Conversion from time domain to the frequency domain baseband signal.
- Removal of the cyclic prefix attached to the signal.
- After removing the cyclic prefix, discrete Fourier transform is performed on the above signal.

The channel model is created using the matrix-based technique, in which the signal from different users is superimposed with the BS signal. The signal received by the user is indicated (15):

$$\begin{aligned} w_{m,n} &= \sum_{bs=1}^{BS} w_{bs,m,n} + Z_{bs,n} = \sum_{bs=1}^{BS} \sum_{j=1}^{M} \left( CH^{H}_{bs,m,n} + \sum_{ris=1}^{R} E^{CH}_{ris,m,n} \odot^{CH}_{ris} G_{bs,ris,n} \right) V_{bs,n,j} D_{n,j} + Z_{bs,n} = \\ &\sum_{bs=1}^{BS} \left( CH^{H}_{bs,m,n} + \sum_{ris=1}^{R} E^{CH}_{ris,m,n} \odot^{CH}_{ris} G_{bs,ris,n} \right) V_{bs,n,m} D_{n,m} + \\ &\sum_{bs=1}^{BS} \sum_{j=1,j \neq m}^{M} \left( CH^{H}_{bs,m,n} + \sum_{ris=1}^{R} E^{CH}_{ris,m,n} \odot^{CH}_{ris} G_{bs,ris,n} \right) V_{bs,n,j} D_{n,j} + Z_{bs,n} \end{aligned} \quad (15)$$

The user required signal without noise and the undesired signal are called interference. The signal from the other users is considered as noisy signal or undesired signal and is represented in (16):

$$\sum_{bs=1}^{BS} \sum_{j=1,j \neq m}^{M} \left( CH^{H}_{bs,m,n} + \sum_{ris=1}^{R} E^{CH}_{ris,m,n} \odot^{CH}_{ris} G_{bs,ris,n} \right) V_{bs,n,j} D_{n,j} + Z_{bs,n} \quad (16)$$

## V. RESULTS AND DISCUSSION

### A. WSR Comparison with Distance for an Ideal RIS and an RIS with Continuous Phase Shift

Performance measures such as sum rate, SINR, energy efficiency, and transmit power were used to analyze and validate the proposed system. The weighted sum rate is compared with distance in meters for an ideal RIS and continues phase shift as depicted in Figure 4. The WSR fluctuates with distance. It can be seen in the graph that the WSR peaks at 13 bits/s/Hz at distances of 60 m and 100 m.

### B. WSR Comparison with Distance for an RIS with Continuous Phase Shift and Random Phase Shift

The continuous phase shift achieves more WSR than random phase shift. Network capacity and deployment can be enhanced with continuous phase shift. The obtained WST peak is 13 at 60 m and 110 m distances as depicted in Figure 5. In random phase shift, the iterations carried out are more hence WSR peak is lesser as compared to the continuous phase shift.

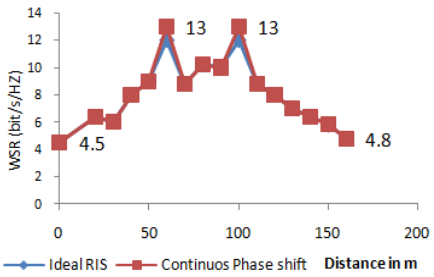


Fig. 4. WSR comparison vs distance for an ideal RIS and an RIS with continuous phase shift.

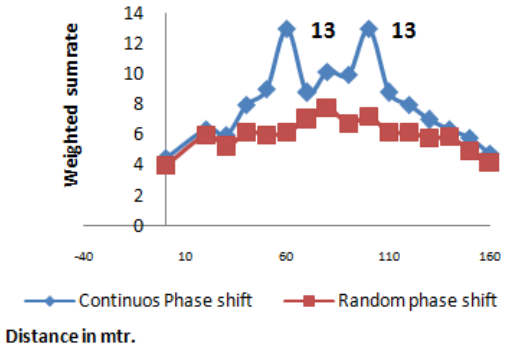


Fig. 5. WSR comparison vs distance for ISRs with continuous and random phase shift.

### *C. WSR Comparison with Distance for an Ideal RIS and without an RIS*

The results with and without a reflecting surface are depicted in Figure 6. The WSR notified is minimum, when the BS propagates the signal to the mobile user directly without super-imposing the signal with an RIS reflected signal. With an ideal RIS, the peak WSR achieved is maximum with a value of 13 bits/s/Hz at 60 m and 100 m.

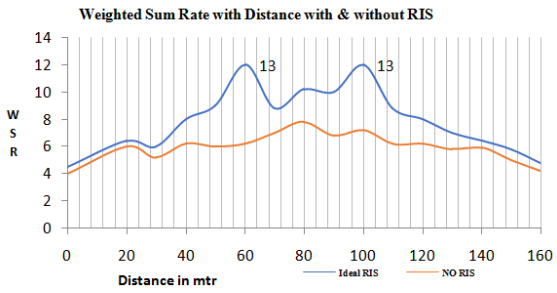


Fig. 6. WSR comparison with distance for an ideal RIS and without an RIS.

### *D. WSR Comparison with Distance for Ideal RIS,without RIS, and with No-Direct Path*

The WSR is compared with the distance in m with an ideal RIS, without RIS, and with no-direct path. Maximum WSR is achieved with an ideal RIS, as depicted in Figure 7.

### *E. WSR vs. Channel State Information Error*

An RIS with continuous phase shift and ideal RIS encounter for 12 iterations are considered. The Channel State Information (CSI) error is comparatively less than 1% due to the increased number of iterations. An RIS with random phase and with no direct path, the number of iterations for WSR converges to around 7, but the CSI error is higher than the previous cases as depicted in Figure 8.


Fig. 7. WSR comparison with distance for an ideal RIS, without RIS, and with no direct path.

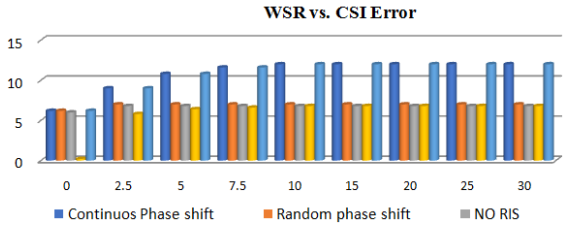


Fig. 8. WSR vs. CSI error.

### *F. WSR vs. CSI Error for 1-bit,2-bit, 3-bit, and 4–bit continuous phase shift*

The WSR with 1, 2, 3, and 4 bit phase shift converges after 1, 8.5, 6, and 4.2 iterations, respectively, as shown in Figure 9.

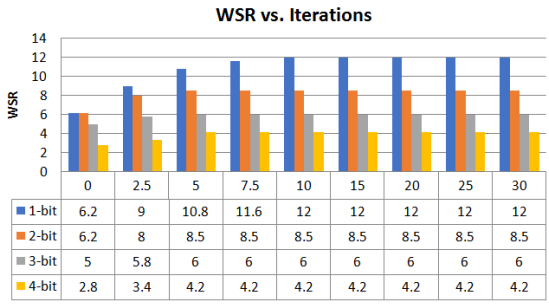


| | 0 | 2.5 | 5 | 7.5 | 10 | 15 | 20 | 25 | 30 |
|---|---|---|---|---|---|---|---|---|---|
| 1-bit | 6.2 | 9 | 10.8 | 11.6 | 12 | 12 | 12 | 12 | 12 |
| 2-bit | 6.2 | 8 | 8.5 | 8.5 | 8.5 | 8.5 | 8.5 | 8.5 | 8.5 |
| 3-bit | 5 | 5.8 | 6 | 6 | 6 | 6 | 6 | 6 | 6 |
| 4-bit | 2.8 | 3.4 | 4.2 | 4.2 | 4.2 | 4.2 | 4.2 | 4.2 | 4.2 |

Fig. 9. WSR vs CSI error for 1-, 2-,3-, and 4-bit continuous phase shift.

The user sum rate is a measure used to compare the performance of massive MIMO and an IRS assisted moderate MIMO communication system. Figure 10 illustrates the sum-rate performance. Initially, it is noticed that the sum-rate performance of an IRS-assisted MIMO system is poorer than that of the massive MIMO system without an IRS. After employing optimal ADMM beam forming technique, the sum-rate obtained in an IRS-assisted MIMO system is significantly higher than that of massive MIMO system without an IRS.

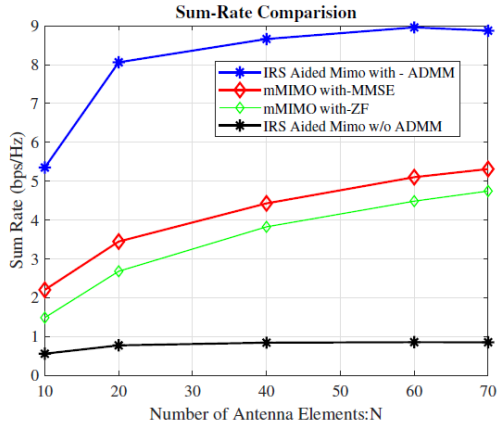


Fig. 10. Sum rate comparison.

As shown in Figure 11, the overall transmit power is reduced significantly by using a large IRS. For example, with 40 reflecting elements, the transmitted power is 4.5 dBm and with 60, the transmitted power is dropped to 2 dBm. As we continually increase the number of reflecting elements to 160 the transmitted power drops to around -11 dBm.

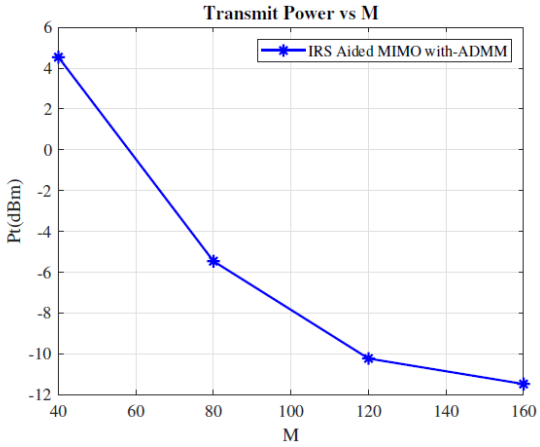


Fig. 11. Transmitted power vs. no. of reflecting elements.

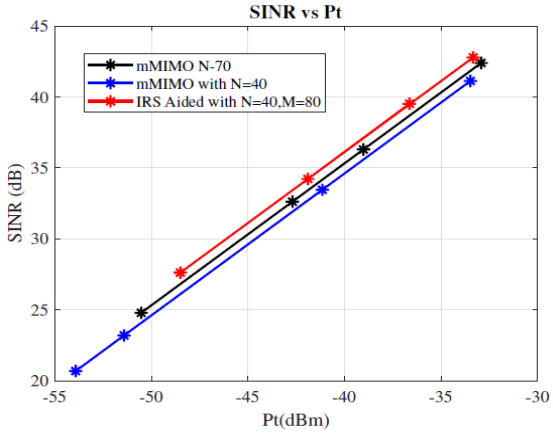


Fig. 12. SINR vs transmitted power.

SINR is the other metric used to compare massive MIMO with the IRS-assisted moderate MIMO communication system. We examine the network SINR achieved by the following three schemes: N = 40 with M = 80, N = 40, and N = 70, with the total amount of antenna elements at the BS and the total amount of reflecting elements at an IRS respectively being N and M. The number of users is K = 20. As shown in Figure 12, passive IRS elements help to reduce the number of active antennas (N = 40 with M = 80 vs N = 40 and N = 80 without an IRS).

Energy efficiency is another criterion used to compare the performance of IRS-aided moderate MIMO versus massive MIMO without an IRS. As depicted in Figure 13, an IRS aided communication is critical in order to create an energy efficient wireless system (where K=20, N=70 and M=120).

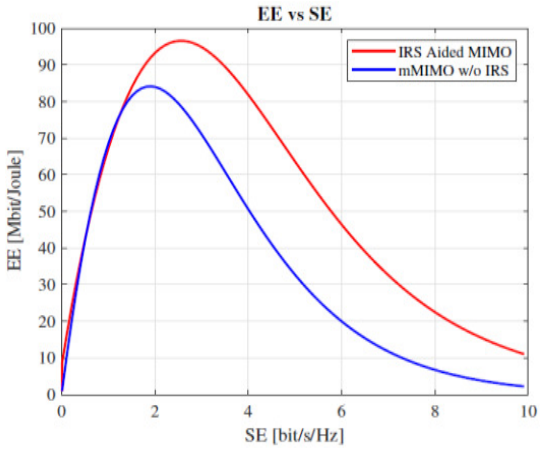


Fig. 13. Energy efficiency vs. spectral efficiency.

## VI. CONCLUSION

In this work, the performance of the cellular free massive MIMO with a reflected intelligent surface is analyzed. Transmitter, receiver, and channel were designed and optimized. The weighted sum rate is plotted with respect to the distance in meters for different phase shift values with an RIS. The WSRs for continuous phase shift RIS, random phase shift RIS, no RIS, ideal RIS, and with direct path are compared. It is noticed with the results that the ideal and with continuous phase shift RISs achieve maximum WSR. Deployment and converge capacity increase with these two techniques. With random phase shift, the obtained peak WSR is 6.2 bits/s/Hz, whereas with continuous phase shift, it is 13 bits/s/Hz. It is concluded that with continuous phase shift, the coverage ratio and the network capacity can be enhanced in a cellular free massive MIMO network. Frame convergence with distance is analyzed, an RIS with continues phase shift converges within 12 iterations, while random phase shift converges within 7 iterations. The system is also analyzed for the cases of no RIS, ideal RIS, and no-direct path. It was noticed that the number of iterations needed for no-RIS and direct path is 6.8. The channel state information error is minimum with continuous phase shift. The error rate with channel state information increases when the number of iterations decreases for random phase shift, no-

RIS, and with no-direct path. WSR converges in 12 iterations for 1-bit, 8.5 iterations for 2-bit, 6 iterations for 3-bit, and 4.2 iterations for 4-th bit phase shift. The CSI error percentage increases with bit size.

The results show that an RIS incorporated cellular free network enhances the coverage and hence more subscribers are able to access the existing infrastructure with reliability than the conventional transmission. RIS will undoubtedly be developed as a promising foundational technology for 6G wireless communication. An IRS-aided system does not have satisfactory results compared to massive MIMO system. We have two different beam-forming schemes, the first is active beam forming at the access point and the second is inactive reflecting beam forming at an IRS. So, we proposed an ADMM algorithm to jointly optimize the two beam forming schemes and concluded that an IRS-aided moderate MIMO system supports maximum users with higher SINR and energy efficiency and lower transmit power than its counterpart without an IRS. IRS-aided MIMO has proven to be very effective in improving the efficiency of a massive MIMO system.

## REFERENCES

[1] C. Huang *et al.*, "Holographic MIMO Surfaces for 6G Wireless Networks: Opportunities, Challenges, and Trends," *IEEE Wireless Communications*, vol. 27, no. 5, pp. 118–125, Oct. 2020, https://doi.org/10.1109/MWC.001.1900534.

[2] W. Saad, M. Bennis, and M. Chen, "A Vision of 6G Wireless Systems: Applications, Trends, Technologies, and Open Research Problems," *IEEE Network*, vol. 34, no. 3, pp. 134–142, Feb. 2020, https://doi.org/10.1109/MNET.001.1900287.

[3] J. Lyu and R. Zhang, "Hybrid Active/Passive Wireless Network Aided by Intelligent Reflecting Surface: System Modeling and Performance Analysis," *IEEE Transactions on Wireless Communications*, vol. 20, no. 11, pp. 7196–7212, Aug. 2021, https://doi.org/10.1109/TWC.2021.3081447.

[4] E. Gures, I. Shayea, A. Alhammadi, M. Ergen, and H. Mohamad, "A Comprehensive Survey on Mobility Management in 5G Heterogeneous Networks: Architectures, Challenges and Solutions," *IEEE Access*, vol. 8, pp. 195883–195913, 2020, https://doi.org/10.1109/ACCESS.2020.3030762.

[5] A. M. S. Abdelgader, S. Feng, and L. Wu, "On channel estimation in vehicular networks," *IET Communications*, vol. 11, no. 1, pp. 142–149, 2017, https://doi.org/10.1049/iet-com.2016.0577.

[6] H. Zhang and H. Dai, "Cochannel Interference Mitigation and Cooperative Processing in Downlink Multicell Multiuser MIMO Networks," *EURASIP Journal on Wireless Communications and Networking*, vol. 2004, no. 2, pp. 1–14, Dec. 2004, https://doi.org/10.1155/S1687147204406148.

[7] M. K. Karakayali, G. J. Foschini, and R. A. Valenzuela, "Network coordination for spectrally efficient communications in cellular systems," *IEEE Wireless Communications*, vol. 13, no. 4, pp. 56–61, Dec. 2006, https://doi.org/10.1109/MWC.2006.1678166.

[8] A. Wiesel, Y. C. Eldar, and S. Shamai, "Linear precoding via conic optimization for fixed MIMO receivers," *IEEE Transactions on Signal Processing*, vol. 54, no. 1, pp. 161–176, Jan. 2006, https://doi.org/10.1109/TSP.2005.861073.

[9] S. Shi, M. Schubert, and H. Boche, "Downlink MMSE Transceiver Optimization for Multiuser MIMO Systems: MMSE Balancing," *IEEE Transactions on Signal Processing*, vol. 56, no. 8, pp. 3702–3712, Dec. 2008, https://doi.org/10.1109/TSP.2008.920487.

[10] M. S. BenSaleh, R. Saida, Y. H. Kacem, and M. Abid, "Wireless Sensor Network Design Methodologies: A Survey," *Journal of Sensors*, vol. 2020, Jan. 2020, Art. no. e9592836, https://doi.org/10.1155/2020/9592836.

[11] M. Amiri and A. Akhavan, "A Novel Detector based on Compressive Sensing for Uplink Massive MIMO Systems," *Journal of Information Systems and Telecommunication (JIST)*, vol. 4, no. 40, Oct. 2022, Art. no. 249, https://doi.org/10.52547/jist.34192.10.40.249.

[12] A. Mirzaei and S. Zandian, "A Novel Approach for Establishing Connectivity in Partitioned Mobile Sensor Networks using Beamforming Techniques," *Journal of Information Systems and Telecommunication (JIST)*, vol. 4, no. 40, pp. 300-311, Oct. 2022, Art. no. 2021061216302, https://doi.org/10.52547/jist.16302.10.40.300.

[13] S. M. Albadarn, "The Effect of Pilot Reuse Factor on Massive MIMO Spectral Efficiency," *Engineering, Technology & Applied Science Research*, vol. 13, no. 3, pp. 10703–10707, Jun. 2023, https://doi.org/10.48084/etasr.5605.

[14] S. Sarade and S. Ruikar, "Development of Two UWB Multiband MIMO Antennas with Enhanced Isolation and Cross-Correlation," *Engineering, Technology & Applied Science Research*, vol. 13, no. 1, pp. 9893–9898, Feb. 2023, https://doi.org/10.48084/etasr.5422.

[15] H. Alsaif, "Extreme Wide Band MIMO Antenna System for Fifth Generation Wireless Systems," *Engineering, Technology & Applied Science Research*, vol. 10, no. 2, pp. 5492–5495, Apr. 2020, https://doi.org/10.48084/etasr.3413.

[16] F. D. Mekonnen, M. M. Tulu, and S. F. Meko, "Performance Analysis of Large Intelligent Reflecting Surface Aided Moderate MIMO for 5G Communication," *Wireless Personal Communications*, vol. 131, no. 2, pp. 1033–1049, Jul. 2023, https://doi.org/10.1007/s11277-023-10467-4.